


ORIGINAL WORK



Neuroprotective Effects of Inhaled Xenon Gas on Brain Structural Gray Matter Changes After Out-of-Hospital Cardiac Arrest Evaluated by Morphometric Analysis: A Substudy of the Randomized Xe-Hypotheca Trial

Carita Hollmén^{1†}, Riitta Parkkola^{1†}, Victor Vorobyev¹, Jani Saunavaara², Ruut Laitio³, Olli Arola³, Marja Hynninen⁴, Minna Bäcklund⁴, Juha Martola⁵, Emmi Ylikoski⁴, Risto O. Roine⁶, Marjaana Tiainen⁷, Harry Scheinin³, Mervyn Maze⁸, Tero Vahlberg⁹ and Timo T. Laitio^{3*} 

© 2024 Springer Science+Business Media, LLC, part of Springer Nature and Neurocritical Care Society

Abstract

Background: We have earlier reported that inhaled xenon combined with hypothermia attenuates brain white matter injury in comatose survivors of out-of-hospital cardiac arrest (OHCA). A predefined secondary objective was to assess the effect of inhaled xenon on the structural changes in gray matter in comatose survivors after OHCA.

Methods: Patients were randomly assigned to receive either inhaled xenon combined with target temperature management (33 °C) for 24 h ($n = 55$, xenon group) or target temperature management alone ($n = 55$, control group). A change of brain gray matter volume was assessed with a voxel-based morphometry evaluation of high-resolution structural brain magnetic resonance imaging (MRI) data with Statistical Parametric Mapping. Patients were scheduled to undergo the first MRI between 36 and 52 h and a second MRI 10 days after OHCA.

Results: Of the 110 randomly assigned patients in the Xe-Hypotheca trial, 66 patients completed both MRI scans. After all imaging-based exclusions, 21 patients in the control group and 24 patients in the xenon group had both scan 1 and scan 2 available for analyses with scans that fulfilled the quality criteria. Compared with the xenon group, the control group had a significant decrease in brain gray matter volume in several clusters in the second scan compared with the first. In a between-group analysis, significant reductions were found in the right amygdala/entorhinal cortex ($p = 0.025$), left amygdala ($p = 0.043$), left middle temporal gyrus ($p = 0.042$), left inferior temporal gyrus ($p = 0.008$), left parahippocampal gyrus ($p = 0.042$), left temporal pole ($p = 0.042$), and left cerebellar cortex ($p = 0.005$). In the remaining gray matter areas, there were no significant changes between the groups.

Conclusions: In comatose survivors of OHCA, inhaled xenon combined with targeted temperature management preserved gray matter better than hypothermia alone.

*Correspondence: timo.laitio@varha.fi

†Carita Hollmén and Riitta Parkkola have equal contribution to this work.

³ Division of Perioperative Services, Intensive Care Medicine and Pain Management, Turku University Hospital, University of Turku, POB 52, 20521 Turku, Finland

Full list of author information is available at the end of the article

Clinical trial registration: ClinicalTrials.gov: NCT00879892.

Keywords: Xenon, Neuroprotection, Out-of-hospital cardiac arrest, Targeted temperature management, Gray matter injury, Voxel-based morphometry

Introduction

The mortality of successfully resuscitated patients with out-of-hospital cardiac arrest (OHCA) remains slightly under 80% [1, 2]. Earlier international guidelines proposed the implementation of a target temperature management (TTM) of 33 °C for comatose survivors of OHCA [3, 4]. Current guidelines recommend avoiding fever (<37.7 °C) for at least 72 h after the return of spontaneous circulation (ROSC) [5]. Guidelines are based on recent large-scale studies, which revealed that the prevention of fever (≥ 37.7 °C) through TTM was as neuroprotective as a TTM between 33 and 36 °C, regardless of the initial rhythm at the time of the OHCA [6, 7].

The leading cause of morbidity and mortality after OHCA is a hypoxic-ischemic brain injury, with survivors at risk of a diverse combination of severe white and gray matter damage [8]. Numerous earlier preclinical studies have confirmed xenon's neuroprotective effect [9–17]. Subsequently, we reported that xenon combined with a TTM of 33 °C conferred neuroprotection by attenuating the injury to brain white matter in comatose survivors of OHCA more effectively than achieving a TTM of 33 °C alone [18]. However, xenon's possible neuroprotective effect on brain gray matter has not been demonstrated in humans. One characteristic of the ischemic damage occurring in humans is that the vulnerability of gray matter varies depending on a metabolic level, with the most susceptible areas being the pyramidal neurons in the CA1 hippocampal region and cerebellar Purkinje cells [3, 19–21]; these areas have important roles in forming memories and coordinating motor activity, respectively [22, 23]. In addition, several investigators have detected a reduction of gray matter volume after the global ischemia [24–26].

The purpose of this study was to investigate xenon's effect on the volumetric changes in brain gray matter in comatose survivors of OHCA at two different time points by applying a voxel-based morphometry technique to evaluate high-resolution structural magnetic resonance imaging (MRI) data.

Methods

Study Design

The Xe-Hypotheca trial was a randomized two-group single-blinded phase II clinical drug trial performed in two multipurpose intensive care units in Finland; the trial was performed at Turku University Hospital between

August 2009 and September 2014 and at Helsinki University Hospital between October 2012 and September 2014. The trial was primarily designed as a proof-of-concept study to investigate whether xenon exerted a neuroprotective effect on human brain white matter after the global ischemia due to OHCA.

The study was approved by the ethics committee of the Hospital District of Southwest Finland on March 17, 2009 (approval number 10/2009/§65) and the institutional review boards of Helsinki University Hospital and the Finnish Medicines Agency. All patients' next of kin or legal representatives gave written informed assent within 4 h after hospital arrival. The patient's family was informed about the right to withdraw from the study at any point but that the data collected until possible withdrawal could be used in the analyses as predefined in the trial protocol [18]. Informed consent was obtained from all individual participants included in the study if they regained consciousness. Clinical investigators performed the patient enrollment, randomization, and intervention assignment. A brain computed tomography scan was performed for all patients before initiation of any treatments to exclude a possible cerebral origin of the cardiac arrest. An independent data and a safety monitoring committee reviewed the data after the enrollment of every four patients and after an interval of 6 months. The study was conducted according to good clinical practice and the latest revision of the Declaration of Helsinki guiding clinical drug research in human study participants.

Patients were allocated in 1:1 ratio with random block sizes of four, six, and eight to receive either TTM (33 °C) alone for 24 h or inhaled xenon (LENOXe; Air Liquide Medical GmbH, Dusseldorf, Germany) with a subanesthetic target concentration of 40% in oxygen/air combined with TTM (33 °C) for 24 h. The treatment assignment was randomly generated by a computer. Sequentially numbered sealed envelopes were used separately in the two centers for randomization, which was performed after the assent was granted.

Treatment Protocol

There was adherence to the detailed treatment protocol regarding cooling treatment and xenon intervention [18]. Hypothermia was induced and maintained with an invasive catheter-based cooling device. Inhaled xenon was initiated immediately after randomization through a closed-system ventilator (PhysioFlex, Dräger); this

had to be initiated within 4 h after hospital admission. Oxygen and air were delivered to achieve an end-tidal xenon concentration of at least 40% (measured continuously by the thermoconductive monitor on the ventilator). The protocol has been published earlier [18].

Patients

In the Xe-Hypotheca trial, consecutive comatose survivors of OHCA were screened for the following inclusion criteria: (1) witnessed cardiac arrest, (2) ventricular fibrillation, (3) nonperfusing ventricular tachycardia, (4) presumed cardiac origin, (5) age 18–80 years, (6) start of resuscitation by emergency medical personnel within 15 min, (7) ROSC within 45 min, (8) decision for therapeutic hypothermia treatment by attending physician. Patients were excluded according to the following criteria: (1) hypothermia (core temperature < 30 °C), (2) unconsciousness before collapse (cerebral trauma, intoxication, etc.), (3) computer tomography scan indicating cerebral pathological reason for cardiac arrest, (4) responding to verbal commands after ROSC, (5) pregnancy, (6) coagulopathy, (7) systolic arterial pressure less than 80 mm Hg lasting > 30 min after ROSC, (8) mean arterial pressure less than 60 mm Hg lasting < 30 min after ROSC, (9) hypoxemia (arterial oxygen saturation < 85%) lasting > 15 min after ROSC, (10) factors making participation in follow-up implausible, and (11) enrollment in another interventional trial. In addition in the current study, patients who underwent each of two MRI scans were considered as being eligible for inclusion. A local neurological prognostication consensus was used in decisions to withdraw life-sustaining treatment, as described in detail in the Supplementary material and in the published protocol [18].

End Points

As a secondary end point in the original protocol the aim of this study was to investigate xenon's effect on the volumetric changes in gray matter after OHCA [18]. The study was not powered to detect statistical differences in clinical efficacy. The following variables were collected at 6 months as exploratory secondary end points of neurological outcome: the Cerebral Performance Category (CPC) score and modified Rankin scale (mRS). The personnel involved in the treatment of the patient could not be masked because of practical and safety considerations, but the neurological end point evaluator and patients were blinded to the treatment. The volumetric analysis of the structural MRI scans was performed by automated operator-independent software.

Imaging Procedure

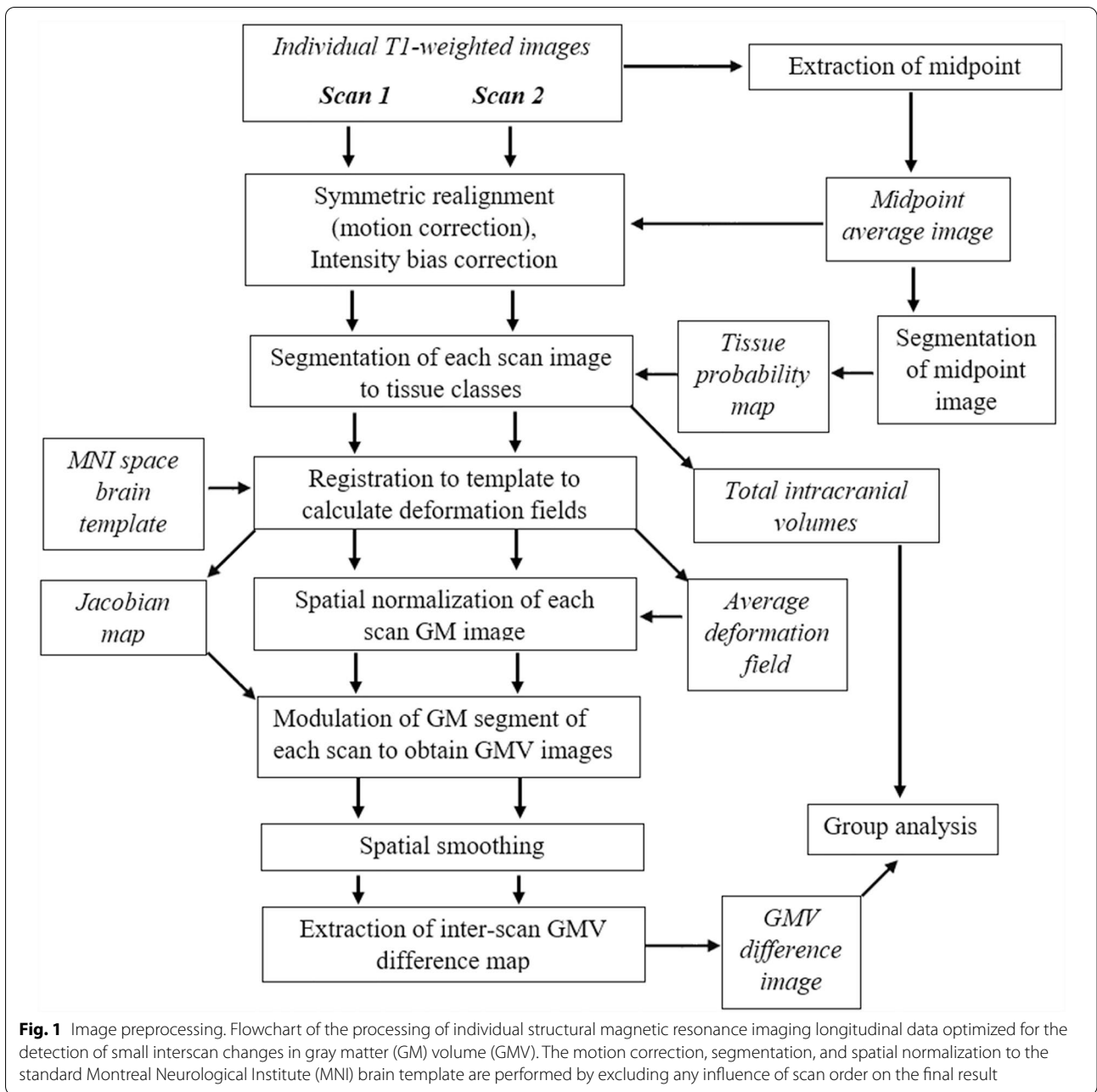
The first brain MRI scan was scheduled 36–52 h and the second scan took place on average at 10 days after the OHCA. Patients were kept intubated and sedated until the first brain scan was performed. In both centers, the structural T1-weighted MRI data were acquired by a 3.0 T Magnetom Verio system (Siemens Healthcare, Erlangen, Germany) equipped with a 12-channel head coil.

A three-dimensional magnetization-prepared rapid gradient-echo sequence was used with a 1900-ms repetition time, 2.2-ms echo time, 900-ms inversion time, 9° flip angle, 200 Hz/Px bandwidth, 250 × 250 × 176 mm³ field-of-view, and 1.0 × 1.0 × 1.0 mm³ resolution. Zero-interpolation filling was applied during image reconstruction so that images had 0.5 × 0.5 × 1.0 mm³ resolution.

The Quality Control and Image Processing

The image processing and quality control (Fig. 1) was performed with the Computational Anatomy Toolbox (CAT12.8.1, Gaser and Dahnke, 2016) of the Statistical Parametric Mapping (SPM12, Version 7771; Wellcome Department of Cognitive Neurology, London, UK; <http://www.fil.ion.ucl.ac.uk/spm>) running under Matlab (R2015a, Mathworks). Structural images of the patients were first inspected visually by two neuroradiologists (RT, CH) to verify their quality and absence of gross anatomical irregularities and head motion artifacts prior to image processing (Figs. 1 and 2).

The MRI data were resliced to a 1-mm³ cubic voxel size and processed according to a variant of the longitudinal pipeline in the CAT12 software (Fig. 1). Thus, for each patient, to be able to correct for differences in between-scan head positions, images from two sequential scans were rigidly registered to a calculated midpoint image using inverse-consistent (symmetric) registration [27]. Therefore, the order of the scans did not influence the number of transformations applied to each image. Images were corrected for bias field inhomogeneity and segmented into the gray matter, white matter, and cerebrospinal fluid tissue classes using average segments as tissue probability maps. The tissue classes were corrected for any partial volume effects. The segmented brain volumes were nonlinearly spatially registered to the brain template in the MNI152 (Montreal Neurological Institute) space using a geodesic shooting algorithm [28]. The deformation parameters calculated at this step for each scan were averaged and the resulting mean deformation was applied to the gray matter images of both scans, thus making the processing pipeline optimized for capturing smaller gray matter changes over short time. The spatially

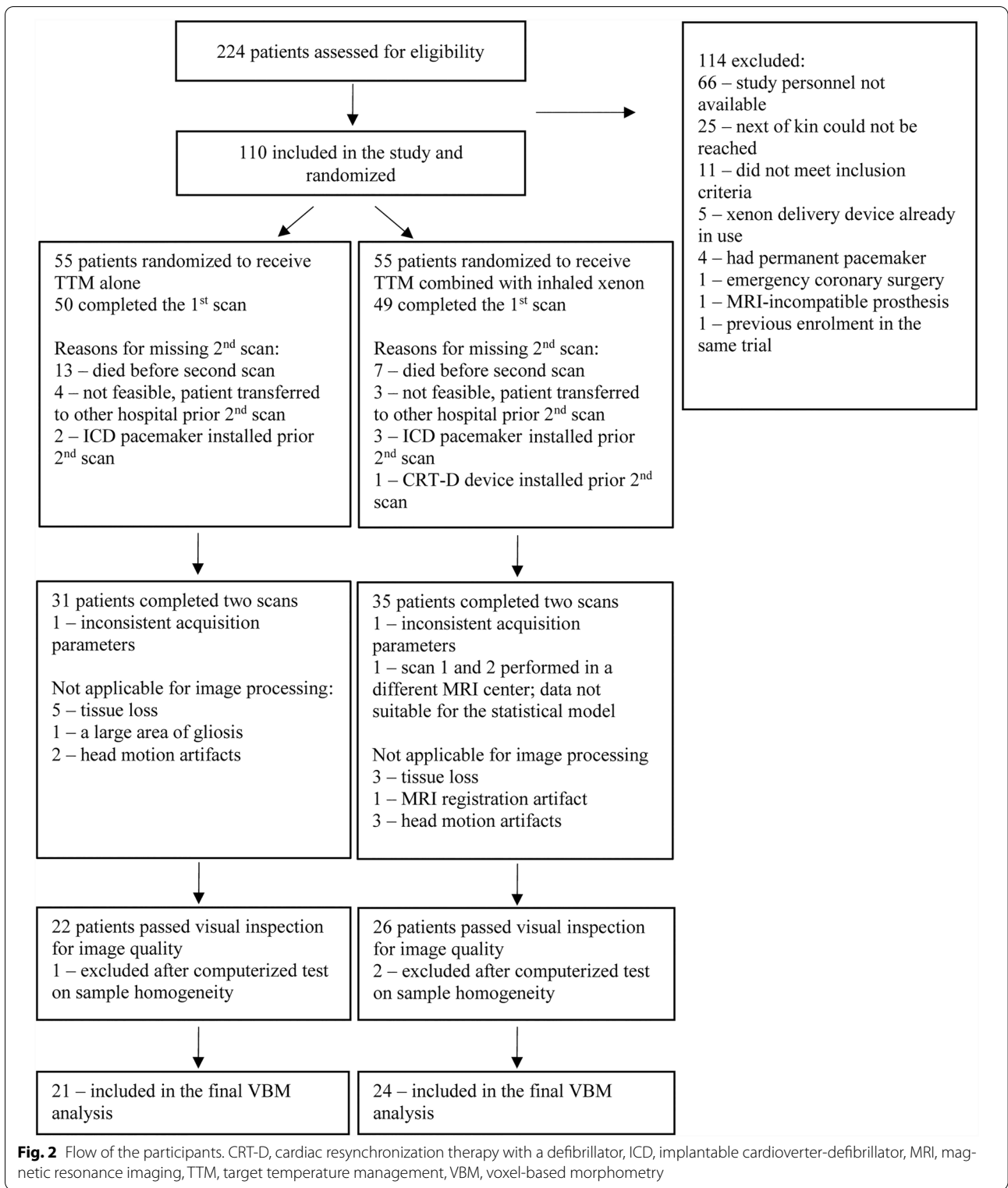


transformed gray matter images were modulated by the Jacobian determinant of the resulting warp to preserve the amount (local volume) of the gray matter signal in the voxels.

The resulting gray matter volume images with 1.5-mm isotropic resolution were smoothed with the 6-mm isotropic Gaussian kernel. All the gray matter images satisfied the weighted overall quality criterion combining mean correlation, bias, and noise, according to the sample homogeneity check function in the CAT12 toolbox.

Statistical Analysis

The sample size of 110 patients was based on a power analysis of the fractional anisotropy values from brain MRI, that is, the primary end point of the Xe-Hypotheca trial [18]. In this study, a between-group difference of gray matter volume changes between the first and second scan was calculated. After image processing (Fig. 1), the gray matter image of the second scan was subtracted from the gray matter image of the first scan, resulting in a difference gray matter image for every patient. These



difference images were entered into a group statistical model with two groups (control and xenon) and confounding covariates of age, gender, and site. The total

intracranial volume of gray matter, white matter, and cerebrospinal fluid was measured for each scan and was included in the model to correct for differences in the

estimated brain size between the scans and to enable the detection of relative, rather than absolute gray matter volume changes. The statistical model was built and estimated with the SPM12 software.

All analyses were spatially constrained by a gray matter mask created by thresholding the 6-mm smoothed average gray matter image with the value of 0.3. The observed effects were assessed with the nonparametric threshold-free cluster enhancement method, which was based on a combination of voxel-level and cluster-level estimations while using 5000 permutations to compute the null distribution [29]. The significance threshold was set at the $p < 0.05$ level after correction for familywise error rate. The statistical map of each of two opposite contrasts between the control and xenon groups after thresholding for significance was masked with a corresponding within-group contrast used as a minuend in the between-group comparison. For example, a map of the difference between the control group and the xenon group was masked with the positive difference between the first and second scan of the control group. The mask was a binarized result of the parametric t -test with a threshold at the uncorrected voxel-wise of $p < 0.05$. The localization of significant effects was performed with the brain atlas (<http://neuromorphometrics.com>) included in the CAT12 software package (Fig. 1).

The differences between xenon and control groups in terms of demographic characteristics, background morbidity, resuscitation details and clinical outcome were tested with two-sample t -test, Mann–Whitney U -test, χ^2 test or Fisher's exact test. $p < 0.05$ was considered statistically significant. Statistical analyses were performed

using SAS System for Windows (Version 9.4; SAS Institute Inc, Cary, NC).

Results

Of the 66 patients who underwent the first and second scan after the OHCA, 21 patients in the control group and 24 patients in the xenon group had both scans that fulfilled the quality criteria and were included in the current final gray matter volume analysis (Fig. 2). The first and second scans were conducted at a median of 51 h (interquartile range [IQR] 46–56 h) and in a median of 10 (IQR 9–11) days, respectively. The mean end-tidal xenon concentration was 48.6% (standard deviation 3.5%) and the range was 43.7% to 56.8%. No differences between treatment groups were detected in demographical data or resuscitation details (Table 1).

The groups were not balanced in respect of neurological outcome (Table 2) after exclusions because of the strict quality reasons (Figs. 1 and 2). In the control group, two patients were initially able to go through the second scan before death, but none of them had an acceptable image quality and were excluded from the current gray matter volume analysis. In the xenon group, seven patients were initially able to undergo the second scan before death and in four of them, the scanned images were of an acceptable quality, and thus they were included in the final gray matter volume analysis. This resulted in significantly different neurological outcome between the groups as assessed with the mRS (median score of 0.5 [IQR 0–2] for the xenon group and 0 [IQR 0–0] for the control group; $p = 0.04$) and CPC (median score of 1.0 [IQR 1–2] for the xenon group and 1.0 [IQR 1–1] for the control group;

Table 1 Demographic data and clinical characteristics of the patients

	Control group (n = 21)	Xenon group (n = 24)	p value
Baseline characteristics			
Age, years, median (IQR)	56 (53–61)	60 (45–67)	0.46
Male sex, n (%)	16 (76)	14 (58)	0.20
Site (Turku/Helsinki)	17/4	17/7	0.50
Coronary artery disease, n (%)	4 (19)	7 (29)	0.43
Hypertension, n (%)	6 (29)	9 (38)	0.53
Congestive heart failure, n (%)	0 (0)	3 (13)	0.24
Diabetes, n (%)	0 (0)	1 (4)	1.00
Asthma or obstructive pulmonary disease, n (%)	1 (5)	4 (17)	0.35
Dyslipidemia, n (%)	7 (33)	4 (17)	0.19
Resuscitation details			
Bystander resuscitation, n (%)	13 (62)	16 (67)	0.74
Delay in EMS, minutes, mean (SD)	8.3 (2.2)	7.9 (2.6)	0.58
ROSC, minutes, mean (SD)	22.2 (7.8)	19.0 (6.3)	0.13
No flow, minutes, median (IQR)	2.90 (0–6)	2.70 (0–7)	0.76

EMS: emergency medical service, IQR, interquartile range, ROSC, return of spontaneous circulation, SD, standard deviation

Table 2 Neurological outcome

		Control group (n = 21)	Xenon group (n = 24)
Cerebral Performance Category score			
1	Good cerebral performance: conscious, alert, able to work, might have mild cognitive deficit	19 (90.5)	16 (66.7)
2	Moderate cerebral disability: conscious, sufficient cerebral function for independent daily life	2 (9.5)	4 (16.7)
3	Severe cerebral disability: conscious, dependent on others for daily support; ranges from ambulatory state to severe dementia	0	0
4	Coma or vegetative state	0	0
5	Death	0	4 (16.7)
Modified Rankin Scale score			
0	No symptoms	16 (76.2)	12 (50.0)
1	No significant disability: able to carry out all usual activities, despite some symptoms	3 (14.3)	3 (12.5)
2	Slight disability: able to look after own affairs without assistance, but unable to carry out all previous activities	1 (4.8)	4 (16.7)
3	Moderate disability: requires some help, but able to walk unassisted	1 (4.8)	1 (4.2)
4	Moderately severe disability: unable to attend to own bodily needs without assistance	0	0
5	Severe disability: requires constant nursing care and attention	0	0
6	Death	0	4 (16.7)

Data are expressed as No. (%). The Cerebral Performance Category and modified Rankin Score differed significantly between the xenon group and the control group ($p=0.04$ for both). See more details in the Results section

$p=0.04$) (Table 2). All patients were sedated and intubated during the first scan. Six patients (five in the xenon group and one in the control group), including the four nonsurvivors, were comatose and intubated during the second scan. All other patients were conscious during the second scan.

In the voxel-based morphometry data, a comparison between the xenon and control group revealed several clusters where the reduction in the local gray matter volume was significantly (familywise error rate corrected $p < 0.05$, threshold-free cluster enhancement statistics) greater from the first to second scan in the control group as compared with the xenon group. The main peak of the largest cluster was found in the left cerebellum. The affected left posterior temporal cortex included the inferior temporal and parahippocampal gyri. The amygdalar nuclei demonstrated bilateral effect with additional involvement of the right entorhinal cortex. Two small clusters were found in middle temporal and polar parts of the left hemisphere. The volumes, peak locations in the standard brain space, and statistical values of the clusters are listed in Table 3. The exact position and extent of the clusters are shown in Fig. 3 as a series of axial brain slices crossing the cluster peaks. The opposite group comparison revealed no significantly greater gray matter volume reduction in the xenon group as compared with the control group.

Discussion

The main finding was that in comatose survivors of cardiac arrest, xenon in combination with TTM preserved gray matter volume better than TTM alone when assessed at a 1-week time interval. This was reflected by significant volumetric reductions evident from the first to second scan in bilateral amygdala and right entorhinal cortex, left inferior and middle temporal gyrus, left temporal pole, left parahippocampal gyrus, and left cerebellar cortex in the control group as compared with the xenon group when we conducted a between-group analysis. There were no significant changes between the groups in the remaining gray matter areas.

In animal studies, the neuroprotective effect of inhalation of the noble gas, xenon, has been confirmed; there are several preclinical studies demonstrating that xenon targets multiple pathophysiologic processes, which are also involved in the development of postresuscitation brain injuries, such as glutamate excitotoxicity, oxidative injury, and neuroapoptosis [9–13]. In addition, neuroprotection has been demonstrated in various injury models involving mice, rats, and pigs, for example, as a reduced infarct volume after a focal ischemia, attenuated neurologic and neurocognitive dysfunction, and a reduction in the extent of the histopathological damage [14–17].

A delayed cell death over a period of hours to days has been demonstrated in selectively vulnerable neuron subpopulations of hippocampus, cortex, amygdala, striatum,

Table 3 Significant clusters with a greater gray matter volume loss in the control group in comparison to the xenon group

Brain structure	cluster size (voxels)	P corr	TFCE value	x	y	z
Left cerebellum exterior	441	0.005	1354.1	-38	-39	-32
Left inferior temporal gyrus		0.008	1268.62	-45	-41	-27
Left parahippocampal gyrus		0.042	854.16	-27	-26	-26
Right amygdala / entorhinal area	223	0.025	979.35	27	0	-18
Right entorhinal area		0.046	831.3	18	2	-29
Left middle temporal gyrus	77	0.042	854.93	-68	-38	-3
Left middle temporal gyrus		0.042	854.75	-65	-47	-8
Left middle temporal gyrus		0.046	830.39	-65	-53	-2
Left temporal pole	56	0.042	852.8	-26	2	-44
Left temporal pole		0.046	829.99	-30	9	-47
Left amygdala	34	0.043	844.43	-26	-2	-21

The familywise error rate corrected p values are based on the threshold-free cluster enhancement statistics making the p value depending both on voxel value and on cluster volume. Each voxel in a cluster represents a significant group difference, which maximizes locally forming the highest peak (voxel with maximal effect) and smaller peaks within the cluster. Voxel locations for the main peak (bold font) and for some prominent secondary peaks (regular font) are listed to characterize a cluster extent in terms of brain structure names and Montreal Neurological Institute coordinates (x , y , z). Figure 3 shows a series of axial planes cutting the clusters at the z -coordinates listed here for the main and secondary peaks

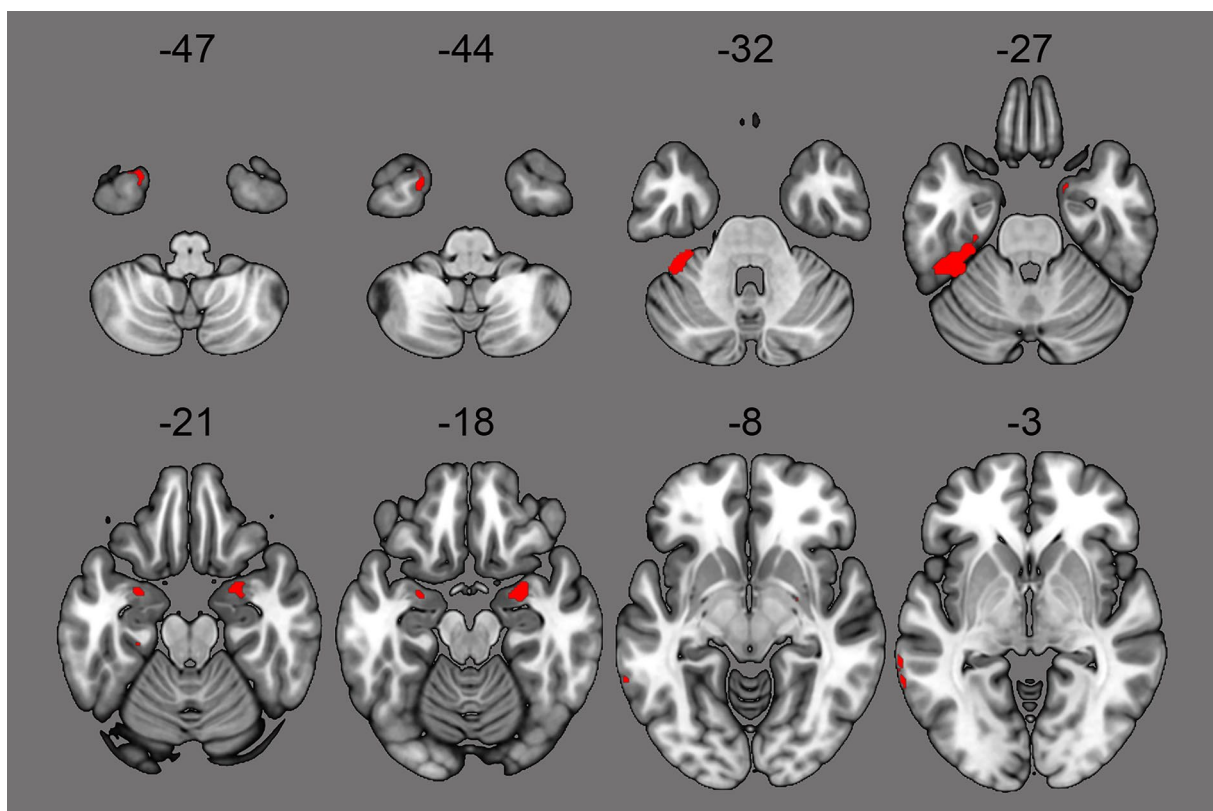


Fig. 3 Clusters where there are significantly (familywise error rate corrected $p < 0.05$, threshold-free cluster enhancement statistics) greater reductions in the local gray matter volume from the first to second scan in in the control group in comparison with the xenon group. The clusters shown are overlaid on brain template axial planes. The numbers denote z -coordinates of the planes in the Montreal Neurological Institute brain space in mm over (positive values) or below (negative values) the intercommissural plane. They correspond to z -coordinates of cluster peaks listed in the Table 3. The right side of the image is the right side of the brain. The main peaks of the significant clusters were located bilaterally in the amygdala, in the right entorhinal cortex, in the left cerebellar cortex, as well as in the middle and inferior temporal gyrus, parahippocampal gyrus, and polar areas of the left temporal cortex. None of the brain areas revealed signs of a significantly greater volume reduction in the xenon group

and cerebellum to global ischemia with apoptosis as a major mode of death [3, 20, 30–34]. This phenomenon may have provided a therapeutic window for xenon and partly explain the drug effect in the observed areas given also xenon's putative ability to attenuate apoptotic cell death [17, 35]. On the other hand, hippocampus is well established to have the highest sensitivity for ischemia-induced brain injury and is the first to show a cellular decline after perfusion deficits and during reperfusion. This is further supported by findings that hippocampal CA1 pyramidal cells and cerebellar granule cells have strong intrinsic glutamatergic and oxidative signaling along with a high demand for energy combined with a low buffering capacity against oxidative stress; these characteristics makes these regions especially vulnerable to excitotoxic cell damage [19–21]. The excitotoxicity is mediated by N-methyl-D-aspartate (NMDA) and α -amino-3-hydroxy-5-methyl-4-isoxazolepropionic acid (AMPA) type glutamate receptors, and glycine is essential for the activation of NMDA receptors [36]. This should be considered with respect to xenon's central mechanism behind its neuroprotective effect; the gas is thought to exert an antagonistic effect on NMDA, AMPA, and kainate glutamate receptors along with competitive inhibition at glycine binding site on the NMDA receptor [9–13].

Xenon's beneficial drug effect was observed on several gray matter areas, including mainly medial temporal lobe memory system [23], in which amygdala directly mediates emotional learning and memory operations. According to earlier trials, approximately 20–50% of patients with OHCA with a good clinical outcome have experienced a mild-to-moderate impairment in cognitive function as assessed with adequately sensitive and accurate tests [37–40]. In addition, earlier studies by Orbo and Stamenova have revealed an association between reductions in the hippocampal volumes and impairment in recollection and recognition in patients with a good clinical outcome after OHCA [24, 25]. Congruently, current findings included volume reductions in the temporomedial area. However, we did not assess higher cognitive function, and therefore it remains unestablished whether xenon exerted any beneficial effect on memory in the current population.

Among nonsurvivors, only seven patients in the xenon group and two patients in the control group were able to undergo the second scan before death. Other succumbing patients in both groups were in a dismal clinical condition already after the OHCA and died prior to the scheduled second scan. In fact, the death rate between the scans was nearly two times higher in the control group. Finally, four patients in the xenon group but none in the control group of those dying after the second scan had an acceptable image quality. This resulted in somewhat

biased imbalance between the groups with respect to the neurological outcome, in which there were nonsurvivors only in the xenon group. Consequently, the mRS and CPC scores were significantly higher in the xenon group than in the control group. It is also important to note that neither the mRS nor CPC scores differed between the groups in the intention-to-treat population of 110 patients [18]. However, even allowing for our inclusion of nonsurvivors in the xenon group, significantly greater reductions in the gray matter were locally observed in the control group as compared with the xenon group.

This study had several limitations. First, the sample size was small, mainly because of the deaths of patients between the scans but also because of quality-related reasons. Second, to avoid systematic errors in the computational image preprocessing only imaging data with a good image quality were accepted, but this can also be considered as a strength. Nevertheless, for these reasons xenon's neuroprotective effect was studied in patients with mainly a good neurological outcome, which probably minimized the differences in gray matter loss between the groups. This was also a likely reason for the relatively small overall brain area of the drug effect and that xenon's benefit was mostly observed in the most vulnerable brain regions. Therefore, current trial may have underestimated the potential treatment effect. Third, this study was not powered to reveal a clinical benefit and did not include neurocognitive tests capable of measuring subtle degrees of functional decline.

Conclusions

Among comatose survivors of OHCA, inhalation of the noble gas, xenon, in combination with TTM preserved gray matter volume better than TTM alone, as measured with a voxel-based morphometric evaluation of high-resolution structural MRI data. The impact of global ischemia on the structural changes occurring in gray matter was demonstrated within 10 days after OHCA in the most vulnerable brain regions. However, no clinical outcome benefit was observed at 6 months, and therefore further studies are warranted in an adequately powered trial designed to evaluate the benefits and risks of xenon administration on neurological outcome and mortality.

Supplementary Information

The online version contains supplementary material available at <https://doi.org/10.1007/s12028-024-02053-8>.

Author details

¹ Department of Radiology, Turku University Hospital, University of Turku, Turku, Finland. ² Department of Medical Physics, Turku University Hospital, University of Turku, Turku, Finland. ³ Division of Perioperative Services, Intensive Care Medicine and Pain Management, Turku University Hospital, University of Turku, POB 52, 20521 Turku, Finland. ⁴ Division of Intensive Care Medicine, Department of Anesthesiology, Intensive Care and Pain Medicine,

Helsinki University Hospital, University of Helsinki, Helsinki, Finland. ⁵ Department of Radiology, Helsinki University Hospital, University of Helsinki, Helsinki, Finland. ⁶ Division of Clinical Neurosciences, Turku University Hospital, University of Turku, Turku, Finland. ⁷ Department of Neurology, Helsinki University Hospital, University of Helsinki, Helsinki, Finland. ⁸ Center for Cerebrovascular Research, Department of Anesthesia and Perioperative Care, University of California, San Francisco, San Francisco, CA, USA. ⁹ Department of Biostatistics, University of Turku and Turku University Hospital, Turku, Finland.

Acknowledgements

We thank research nurses Keijo Leivo (Registered nurse, Turku University Hospital, was compensated for his contribution) and Tuukka Tikka (Registered nurse, Helsinki University hospital, was compensated for his contribution) for taking care of the logistics of this study. The Xe-HYPOTHECA Research Group members included the following: Department of Radiology, University of Turku, Turku University Hospital, Turku, Finland: Sami Virtanen, MD. Heart Center, Turku University Hospital and University of Turku, Turku, Finland: Juhani Airaksinen, MD, PhD; Mikko Pietilä, MD, PhD; Antti Saraste, MD, PhD. University of Turku and Turku University Hospital, Turku, Finland: Juha Grönlund, MD, PhD; Outi Inkinen, MD. Division of Intensive Care Medicine, Department of Anesthesiology, Intensive Care and Pain Medicine, University of Helsinki and Helsinki University Hospital, Helsinki, Finland: Eija Nukarinen, MD; Klaus T. Olkkola, MD, PhD; Johanna Wennervirta, MD, PhD. Emergency Medicine, Department of Emergency Medicine and Services, University of Helsinki and Helsinki University Hospital, Helsinki, Finland: Veli-Pekka Harjola, MD, PhD; Department of Cardiology, Heart and Lung Center, University of Helsinki and Helsinki University Hospital, Helsinki, Finland: Jussi Niiranen, MD; Kirsi Korpi, MD; Marjut Varpula, MD, PhD. Department of Radiology, University of Helsinki and Helsinki University Hospital, Helsinki, Finland: Heli Silvennoinen, MD, PhD.

Author Contributions

TTL had full access to all of the data in the study and takes responsibility for the integrity of the data and the accuracy of the data analysis. TTL, RP and VV: Study concept and design; VV: Image preprocessing; All authors: Acquisition, analysis, or interpretation of the data; CH, RP, VV and TTL: Drafting of the first manuscript; All authors: Critical revision of the manuscript for important intellectual content; TV, VV: Statistical analysis; TTL, ROR: Obtained funding; TTL: Administrative, technical, or material support. The authors approved the final version of the manuscript.

Source of Support

The study was funded by Academy of Finland and by State Research Funding, Finland.

Conflicts of interest

TL reports funding from State Research Funding, Finland. RL is a paid governmental consultant official for the National Supervisory Authority for Welfare and Health. ROR reports funding from the Academy of Finland. For the remaining authors, none were declared.

Ethical Approval/Informed Consent

The study was approved by the ethics committee of the Hospital District of Southwest Finland on March 17, 2009 (approval Number 10/2009/§65; study title: Effect of Xenon, in Combination with Therapeutic Hypothermia, on the Brain and on Neurological Outcome following Brain Ischemia in Cardiac Arrest Patients) and the institutional review boards of Helsinki University Hospital and the Finnish Medicines Agency. All patients' next of kin or legal representatives gave written informed assent within four hours after hospital arrival. Consent was obtained from patients when they regained consciousness.

Publisher's Note

Springer Nature remains neutral with regard to jurisdictional claims in published maps and institutional affiliations.

Springer Nature or its licensor (e.g. a society or other partner) holds exclusive rights to this article under a publishing agreement with the author(s) or other rightsholder(s); author self-archiving of the accepted manuscript version of this article is solely governed by the terms of such publishing agreement and applicable law.

Received: 31 March 2024 Accepted: 14 June 2024

Published online: 09 July 2024

References

1. Kiguchi T, Okubo M, Nishiyama C, et al. Out-of-hospital cardiac arrest across the world: first report from the international liaison committee on resuscitation (ILCOR). *Resuscitation*. 2020;152:39–49.
2. Gräsner JT, Wnent J, Herlitz J, et al. Survival after out-of-hospital cardiac arrest in Europe- results of the EuReCa TWO study. *Resuscitation*. 2020;148:218–26.
3. Nolan JP, Neumar RW, Adrie C, et al. Post-cardiac arrest syndrome: epidemiology, pathophysiology, treatment, and prognostication; a scientific statement from the international liaison committee on resuscitation; the American heart association emergency cardiovascular care committee; the council on cardiovascular surgery and Anesthesia; the council on cardiopulmonary, perioperative, and critical care; the council on clinical cardiology; the council on stroke. *Resuscitation*. 2008;79:350–79.
4. Hypothermia after Cardiac Arrest Study Group. Mild therapeutic hypothermia to improve the neurologic outcome after cardiac arrest. *N Engl J Med*. 2002;346(8):549–56.
5. Sandroni C, Nolan JP, Andersen LW, et al. ERC-ESICM guidelines on temperature control after cardiac arrest in adults. *Intensive Care Med*. 2022;48:261–9.
6. Nielsen N, Wetterslev J, Cronberg T, et al. TTM Trial investigators, targeted temperature management at 33°C versus 36°C after cardiac arrest. *N Engl J Med*. 2013;369(23):2197–206.
7. Dankiewicz J, Cronberg T, Lilja G, et al. Hypothermia versus normothermia after out-of-hospital cardiac arrest. *N Engl J Med*. 2021;384(24):2283–94.
8. Sandroni C, Cronberg T, Sekhon M. Brain injury after cardiac arrest: pathophysiology, treatment, and prognosis. *Intensive Care Med*. 2021;47(12):1393–414.
9. Franks NP, Dickinson R, De Sousa SL, Hall AC, Lieb WR. How does xenon produce anaesthesia? *Nature*. 1998;396(6709):324.
10. Wilhelm S, Ma D, Maze M, Franks NP. Effects of xenon on in vitro and in vivo models of neuronal injury. *Anesthesiology*. 2002;96(6):1485–91.
11. Dinse A, Föhr KJ, Georgieff M, Beyer C, Bulling A, Weigt HU. Xenon reduces glutamate-, AMPA-, and kainate-induced membrane currents in cortical neurones. *Br J Anaesth*. 2005;94(4):479–85.
12. Hasender R, Kratzer MS, Kochs E, Mattusch C, Eder M, Rammes G. Xenon attenuates excitatory synaptic transmission in the rodent prefrontal cortex and spinal cord dorsal horn. *Anesthesiology*. 2009;111:1297–307.
13. Banks P, Franks NP, Dickinson R. Competitive inhibition at the glycine site of the N-methyl-D-aspartate receptor mediates neuroprotection against hypoxia-ischemia. *Anesthesiology*. 2010;112(3):614–22.
14. Thoresen M, Hobbs CE, Wood T, Chakkarapani E, Dingley J. Cooling combined with immediate or delayed xenon inhalation provides equivalent long-term neuroprotection after neonatal hypoxia-ischemia. *J Cereb Blood Flow*. 2009;29(4):707–14.
15. Chakkarapani E, Dingley J, Liu X, et al. Xenon enhances hypothermic neuroprotection in asphyxiated newborn pigs. *Ann Neurol*. 2010;68(3):330–41.
16. Hobbs C, Thoresen M, Tucker A, Aquilina K, Chakkarapani E, Dingley J. Xenon and hypothermia combine additively, offering long-term functional and histopathologic neuroprotection after neonatal hypoxia/ischemia. *Stroke*. 2008;39(4):1307–13.
17. Ma D, Hossain M, Chow A, et al. Xenon and hypothermia combine to provide neuroprotection from neonatal asphyxia. *Ann Neurol*. 2005;58(2):182–93.
18. Laitio R, Hynninen M, Arola O, et al. Effect of inhaled xenon on cerebral white matter damage in comatose survivors of out-of-hospital cardiac arrest. *JAMA*. 2016;315(11):1120–8.
19. Wilde GJ, Pringle AK, Wright P, Iannotti F. Differential vulnerability of the CA1 and CA3 subfields of the hippocampus to superoxide and hydroxyl radicals in vitro. *J Neurochem*. 1997;69:883–6.
20. Einenkel A-M, Salameh A. Selective vulnerability of hippocampal CA1 and CA3 pyramidal cells: What are possible pathomechanisms and should

-
- more attention be paid to the CA3 region in future studies? *J Neurosci Res.* 2023;102:e25276.
21. Wang X, Zaidi A, Pal R, et al. Genomic and biochemical approaches in the discovery of mechanisms for selective vulnerability to oxidative stress. *BMC Neurosci.* 2009;19(10):12.
 22. Wixted JT, Squire LR. Recall and recognition are equally impaired in patients with selective hippocampal damage. *Cog, Affect, and Behav Neurosci.* 2004;4(1):58–66.
 23. LaBar KS, Cabeza R. Cognitive neuroscience of emotional memory. *Nature Rev Neurosci.* 2006;7:54–64.
 24. Ørbo M, Vangberg TR, Tande PM, Anke A, Aslaksen PM. Memory performance, global cerebral volumes and hippocampal subfield volumes in long-term survivors of out-of-hospital cardiac Arrest. *Resuscitation.* 2018;126:21–8.
 25. Stamenova V, Nicola R, Aharon-Peretz J, Goldsher D, Kapeliovich M, Gilboa A. Long term effects of brief hypoxia due to cardiac arrest: Hippocampal reductions and memory deficit. *Resuscitation.* 2018;126:65–71.
 26. Silva S, Peran P, Kerhuel L, et al. Brain gray matter MRI morphometry for neuroprognostication after cardiac arrest. *Critical Care Med.* 2017;45(8):e763-77.
 27. Reuter M, Rosas HD, Fischl B. Highly accurate inverse consistent registration: a robust approach. *Neuroimage.* 2010;53(4):1181–96.
 28. Ashburner J, Friston KJ. Diffeomorphic registration using geodesic shooting and Gauss-Newton optimisation. *Neuroimage.* 2011;55(3):954–67.
 29. Spisák T, Spisák Z, Zunhammer M, et al. Probabilistic TFCE: A generalized combination of cluster size and voxel intensity to increase statistical power. *Neuroimage.* 2019;185:12–26.
 30. Pulsinelli WA, Briery JB, Plum F. Temporal profile of neuronal damage in a model of transient forebrain ischemia. *Ann Neurol.* 1982;11:491–8.
 31. Pulsinelli WA. Selective neuronal vulnerability: morphological and molecular characteristics. *Prog Brain Res.* 1985;63:29–37.
 32. Kurth CD, Priestley M, Golden F, McCann J, Raghupathi R. Regional patterns of neuronal death after deep hypothermic circulatory arrest in newborn pigs. *J Thorac Cardiovasc Surg.* 1999;118:1068–77.
 33. Lipton P. Ischemic cell death in brain neurons. *Physiol Rev.* 1999;79:1431–568.
 34. Taraszewska A, Zelman IB, Ogonowska W, Chrzanowska H. The pattern of irreversible brain changes after cardiac arrest in humans. *Folia Neuro-pathol.* 2002;40:133–41.
 35. Ma D, Hossain M, Pettet GJ, et al. Xenon preconditioning reduces brain damage from neonatal asphyxia in rats. *J Cereb Blood Flow.* 2006;26:199–208.
 36. Yao W, Ji F, Chen Z, et al. Glycine exerts dual roles in ischemic injury through distinct mechanisms. *Stroke.* 2012;43(8):2212–20.
 37. Lilja G, Nielsen N, Friberg H, et al. Cognitive function in survivors of out-of-hospital cardiac arrest after target temperature management at 33°C versus 36°C. *Circulation.* 2015;131(15):1340–9.
 38. Cronberg T, Lilja G, Horn J, et al. Neurologic function and health-related quality of life in patients following targeted temperature management at 33°C vs 36°C after out-of-hospital cardiac arrest. *JAMA Neurol.* 2015;72(6):634–41.
 39. Oreilly SM, Grubb NR, Ocarroll RE. In-Hospital cardiac arrest leads to chronic memory impairment. *Resuscitation.* 2003;58(1):73–9.
 40. Sulzgruber P, Kliegel A, Wandaller C, et al. Survivors of cardiac arrest with good neurological outcome show considerable impairments of memory functioning. *Resuscitation.* 2015;88:120–5.